

## MEASUREMENT OF BASIC HEMODYNAMICS DURING MULTIPOST TRANSCUTANEOUS EXTERNAL EAR STIMULATION: A TWO-CASE STUDY

### MERITEV OSNOVNE HEMODINAMIKE MED VEČTOČKOVNO TRANSKUTANO STIMULACIJO ZUNANJEGA UŠESA: ŠTUDIJA NA DVEH OSEBAH

**Janez Rozman<sup>1,2\*</sup>, Katarina Miklavc<sup>2</sup>, Ingrid Rozman<sup>3</sup>, Anja Emri<sup>4</sup>,  
Tomislav Mirkovič<sup>5</sup>, Samo Ribarič<sup>2</sup>**

<sup>1</sup>Center for Implantable Technology and Sensors, ITIS d. o. o. Ljubljana, Lepi pot 11, 1000 Ljubljana, Slovenia

<sup>2</sup>Institute of Pathophysiology, Faculty of Medicine, University of Ljubljana, Zaloška 4, 1000 Ljubljana, Slovenia

<sup>3</sup>The Family Study and Research Centre, Dvor 12, 1210 Ljubljana-Šentvid, Slovenia

<sup>4</sup>Medical Chamber of Slovenia, Dunajska cesta 162, 1000 Ljubljana, Slovenia

<sup>5</sup>Department of Anaesthesiology and Surgical Intensive Therapy, University Medical Centre Ljubljana, Zaloška 2, 1000 Ljubljana, Slovenia

*Prejem rokopisa – received: 2023-10-26; sprejem za objavo – accepted for publication: 2024-04-04*

doi:10.17222/mit.2023.1032

The objectives of the investigation were to assess the short-term responses of the cardio-vascular system on the multipost transcutaneous stimulation (tANS) of the external ear (EE). The scope was to measure the forefinger photopleths (FPPG), toe photopleths (TPPG), aortic phonocardiogram (APCG), mitral phonocardiogram (MPCG) and brachial arterial blood pressure (BABP), assuming that they could be altered with the tANS. For the tANS, stimulator, two silicone ear plugs with four platinum electrodes each, and a large common electrode (CE), were used. Trials were carried out with two female volunteers, aged 25 years and 28 years. To capture the heart sounds, two customized electronic stethoscopes (transducers) were used. BABP was measured using a pressure transducer and blood-pressure appliance. To measure the FPPGs, a pulse oximeter and SpO2 finger clip were used. To measure the TPPGs, another pulse oximeter and customized SpO2 foot clip was used. Signals were gathered using a high-performance data-acquisition system. An offline analysis was made just before and just after the start of the tANS. To record the pulsations in the right brachial artery, the 2D ultrasound mode (B) of the ultrasound device was used before and during the tANS. Then, diagrams showing the vein cross-sectional area over time were constructed. The results show that vascular time intervals between heart sounds S1 and S2, captured as APCG and systolic peaks of the FPPG in the second volunteer, were slightly larger during the separate tANS of the left white (LW) and (RW) EE post than before the tANS. Furthermore, vascular time intervals between the heart sounds S1 and S2, captured as MPCG and systolic peaks of the TPPG in the second volunteer, were slightly smaller during the separate tANS of LW and RW EE post than before the tANS. Finally, tANS of the LW post elicited a slightly lower heart rate than the one measured when LW was not stimulated. In contrast, the tANS of the RW post elicited a slightly higher heart rate than the one measured when RW was not stimulated. It was also shown that the pattern of the vein cross-sectional area over time with tANS was different compared to both the FPPG and TPPG.

Keywords: external ear stimulation, hemodynamics, measurement, signal acquisition

Cilj raziskave je bil ovrednotiti kratkoročne odzive srčno-žilnega sistema na večtočkovno transkutano stimulacijo (tANS) zunanjskega ušesa (EE). Raziskava je obsegala meritve fotopletizmogramov na palcu desne roke (FPPG), fotopletizmogramov na palcu leve noge (TPPG), aortnih fonokardiogramov (APCG), mitralnih fonokardiogramov (MPCG) in brahialnega arterijskega krvnega tlaka (BABP) predpostavljač, da se bodo spremenili vsled tANS. Za tANS so bili uporabljeni stimulator, dva ušesna čepka iz silikona s po štirimi platinastimi elektrodami in velika skupna elektroda (CE). Meritve so bile opravljene na dveh prostovoljkih starih 25 let in 28 let. Za zajemanje zvokov srca sta bila uporabljena dva posebej izdelana elektronska stetoskopa (transducer). BABP pa je bil merjen s pretvornikom tlaka in merilcem krvnega tlaka. Za meritve FPPG je bil uporabljen pulzni oksimeter z naprtnim SpO2 senzorjem. Za meritve TPPG pa je bil uporabljen drugi pulzni oksimeter s posebnim SpO2 senzorjem na nožnem palcu. Signali so bili digitalizirani z zmogljivim sistemom za zajemanje podatkov. Kasnejša analiza podatkov je bila narejena tik pred začetkom in takoj po končani tANS. Za beleženje pulziranja desne brahijalne arterije je bil uporabljen 2D ultrazvočni način (B) ultrazvočne naprave in sicer pred in med tANS. Nato sta bila konstruirana diagrama, ki sta prikazovala presek arterije v odvisnosti od časa. Rezultati so pokazali, da so bili časovni intervali med zvoki srca S1 in S2 zajeti kot APCG in sistoličnimi vrhi pri drugi prostovoljki, rahlo daljši tako med tANS levega belega (LW) kot tudi desnega (RW) mesta na EE, kot pred tANS. Nadalje so bili časovni intervali med zvoki srca S1 in S2 zajeti kot MPCG in sistoličnimi vrhi pri isti prostovoljki, rahlo krajši tako med tANS levega belega (LW) kot tudi desnega (RW) mesta na EE, kot pred tANS. Razen navedenega je prišlo v času tANS mesta LW do rahlega zmanjšanja frekvenc srčnega utripa kot je bil v času brez tANS. Nasprotno pa je prišlo v času tANS mesta RW do rahlega povečanja ritma srca kot je bil v času brez tANS. Rezultati so tudi pokazali, da je bil časovni potek sprememb površine prereza arterije v odvisnosti od časa med tANS različen tako od poteka FPPG kot tudi od poteka TPPG.

Ključne besede: stimulacija zunanjskega ušesa, hemodinamika, meritve, zajemanje signala

\*Corresponding author's e-mail:  
jnzrzm6@gmail.com (Janez Rozman)

## 1 INTRODUCTION

Electrical nerve stimulation is the most often used technique to provide external control over body systems that are normally under the control of the nervous system.<sup>1</sup> Surgically implanted devices currently used for the stimulation of vagus nerve afferents have many disadvantages. It was presumed, however, that most of them can be overcome using the novel method of transcutaneous vagus nerve stimulation tVNS.<sup>2</sup> Thus, tVNS devices that target the auricular (tANS) portion of the vagus nerve may have the potential to be implemented for rehabilitation, and treatment of physiological and mental disorders.<sup>3</sup> Namely, tANS technology targets afferents within the auricular branch of the vagus nerve that can be accessed from the external ear (EE).<sup>4</sup> Some studies reported effects of the tANS on the regulation of autonomic function through measurements of the heart rate, heart-rate variability, blood pressure, and related physiological quantities in healthy volunteers and in vascular hypertensive patients.<sup>5</sup>

One non-invasive procedure used to describe the heart-function dynamics is phonocardiography (PCG). It is the graphical representation of heart sounds providing information useful to reveal abnormalities in the movement of the heart wall, closure of the valves, or the leakage of blood flow.<sup>6</sup> In this regard, the PCG can be utilized to auscultate and distinguish four sounds during the heart cycle, i.e., S1, S2, S3, and S4, that arise from opening and closing of a valve.<sup>7</sup> Traditional positions of heart auscultation at the thorax are the following: the mitral area above the cardiac apex, the tricuspid area above the fourth and fifth intercostal space along the left sternal border, the pulmonic area above the second intercostal space along the left sternal border and aortic area above the second intercostal space along the right sternal border. Heart sounds are complex and non-stationary subtle body sounds. They can be described by their intensity, pitch, position, quality and timing in the heart cycle.<sup>8</sup> Loudness of the heart is usually measured in decibels (dB) based on how far away a tested person is. To assess the heart function, a heart-sound activity detection framework has been developed by Varghees et al.<sup>9</sup> The authors captured PCG signals that included four heart sounds: S1, S2, S3 and S4. They also identified average heart sound durations, the time delay between heart sounds, and the duration of heart cycles. Finally, they identified normal frequency ranges of heart sounds (S1 (50–150) Hz, S2 (50–200) Hz, S3 (50–90) Hz, and S4 (50–80) Hz). Fast Fourier transform (FFT) was used for automatic heart-sound signal analysis. In healthy subjects, the two heart sounds, S1 and S2, are the most frequently used in the PCG analysis.<sup>10</sup> S1 results from the closing of the mitral and tricuspid valves. The sound produced by the closure of the mitral valve is termed M1, and the sound produced by the closure of the tricuspid valve is termed T1. M1 is the main component of S1 and is much louder than T1. S2, however, is produced by the

closure of the aortic and pulmonic valves where the closure of the aortic valve is termed A2, and the closure of the pulmonic valve is termed P2. A2 is normally much louder than P2 and is the main component of S2. In general, heart valves have been considered passive structures that only function in response to the hemodynamic forces generated by heart contractions.<sup>11</sup> However, under physiological conditions, autonomic sympathetic nerves and the vagus nerve modulate the mechanical properties of heart valves. However, little focus has been given to the regulation of heart valves by the autonomic nervous system.<sup>12</sup> As the mitral valve is exposed to high mechanical forces during each heart cycle, it can be hypothesized that under such physiological conditions, mitral valve tissue stiffness varies in response to autonomic nervous agents and that the leaflet tone and valve function are modulated. Therefore, there is a need to identify the role of the autonomic nerve in the regulation of mitral valve mechanical properties.

Oximeters used in pulse oximetry<sup>13</sup> often provide a patient's heart rate via an assessment of the arterial blood pulsations. Pulse oximeters are also able to visualize a blood-volume change in the tissue caused by the passage of blood, and this is called a plethysmographic trace. It can resemble an arterial pressure waveform and is approximated by the ratio of the stroke volume output to the compliance of the arterial tree. In clinical practice, photoplethysmography (PPG) is routinely used to monitor cardiac-induced blood volume changes at peripheral body sites, such as the finger, forehead, earlobe, and toe.<sup>14</sup> A normal PPG is characterized by a sharp systolic upstroke and peak and by a prominent dicrotic notch on the downward portion of the PPG. With compromised blood flow through an artery, however, the dicrotic notch can be lost or reshaped. A photoplethysmograph is often used to measure an optical PPG. It offers a simple and inexpensive method to detect blood-volume changes in the microvascular bed of tissue and to measure toe blood pressure.<sup>15</sup>

In critically ill or hemodynamically unstable patients, however, there is a frequent need for hemodynamic monitoring such as cardiac output, oxygen saturation, and stroke volume variation. Hemodynamic monitoring is a procedure used in the repeated assessment of circulatory function to check blood circulation and to evaluate how well a heart is working over time.<sup>16</sup> The results of a hemodynamic test demonstrate how much blood a heart can pump and how well blood travels through the blood vessels. They can thus identify problems and suggest possibilities to address them. With this regard, the ultrasound mode that is normally used to study vasculature is the two-dimensional (2-D) (B) mode. It uses the echo from solid structures to display 2-D images of the walls of blood vessels.<sup>17</sup> Data obtained by the most sophisticated duplex ultrasound instrument can show macrovascular features of vascular physiology including imaging and flow velocity profiles.

The present study was aimed at testing whether the multi post tANS of afferent nerve fibres within the auricular branch of the vagus nerve can be used as a method for the external modulation of basic hemodynamic function. The main goal was to identify, record and analyse the short-term responses of the cardio-vascular system on the multipost tANS. The specific goal was to retain the characteristics of the main events within the measured signals and to analyse them if they contained extractable information resulting from the tANS. With regard to the cardio-vascular system, the aim was to measure the forefinger photopleths (FPPG), toe photopleths (TPPG), PCG, and Brachial artery blood pressure (BABP), assuming that all can be altered with the tANS.

## 2 EXPERIMENTAL PART

### 2.1 Protocol Approval, Subject Consent and Subject Health Status

This study was conducted on two female volunteers, aged 25 and 28 years. Anthropometric data for the first volunteer: age 25 years, height 174 cm, weight 63 kg, non-smoker, systolic blood pressure 115 mmHg and heart rate 60/min. Anthropometric data for the second volunteer: age 28 years, height 160 cm, weight 50 kg, non-smoker, systolic blood pressure 110 mmHg and heart rate 56/min. Both were in top physical condition and were free from any known cardio-vascular disease. They were recruited by asking them to participate in the study. Each participant was recruited for the study at different times. We carried out the study approved by the National Medical Ethics Committee, Ministry of Health, Republic of Slovenia (No. 0120-297/2018/6).

### 2.2 Medical isolation and noise reduction

The entire setup was connected to the human by considering the class safety standard (IEC 60601: International Product Safety Standards for Medical Devices). To accomplish the galvanical isolation between the mains supply section and that of the measuring setup section, the highest quality vintage 500 VA isolation transformer (supplied in 1966 with the STM-200-b studio Reel-to-Reel Mono Tape Recorder for professional use, Mechanikai Laboratórium (ML), Budapest, Hungary), was used. The isolation transformer used has a leakage current of 15  $\mu$ A which was within the range of transformers rated for medical applications (between 10 and 50  $\mu$ A). This power supply isolation also enabled a break of the ground loops and thereby the elimination of noise in the measuring setup. To additionally inhibit the noise transmitted through the grid power cable and high-frequency interference signals generated by the electronic device itself, the CE Certified Single-Phase 220V AC, 15A, EMI Power Supply Filter (EMI Filter) with Dual-Stage S Purification (CW4L2-I5A-S, Canny Well

Co., Ltd., No. 333, Jen Chian St., Shu-Lin 23855, Taiwan, China) was used.

### 2.3 Multipost transcutaneous stimulation set-up

For the multi post tANS, the certified microprocessor-controlled stimulator (Model SM9079, Shenzhen L-Domas Technology Ltd., Shenzhen, Guangdong, China) was used. The pattern of the stimuli train was selected from a palette of patterns available with the stimulator. The proprietary stimulating pulse was symmetrical, current-regulated rectangular and dual directional stimulating pulse pair. The parameters selected at the stimulator were the following:

Frequency	$f = 45.5$ Hz,
Stimulating phase width	$t_c = 200$ $\mu$ s,
Anodic phase width	$t_a = 200$ $\mu$ s,
On time (pulse train duration)	3.32 s,
Time gap between pulses train	2.8 s.

To deliver the stimuli to a particular post at the EE, the negative output of the stimulator was connected to the corresponding electrode using a custom-developed switching unit. The common anode (CE), however, was connected to the positive output of the stimulator. For the multipost tANS, the two silicone ear plugs, having four platinum electrodes each, were developed. They were mounted onto the frame of the headphones and inserted

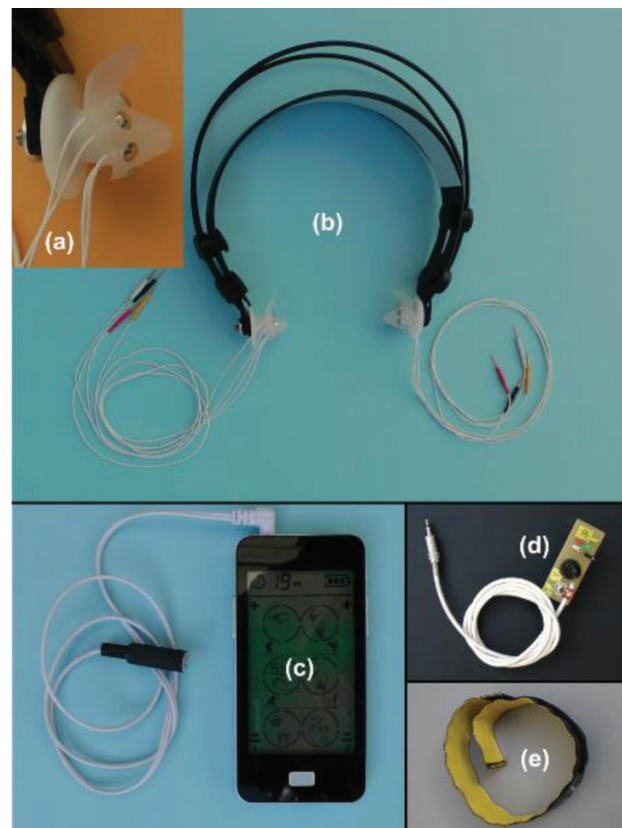


**Figure 1:** Stimulating system: a) stimulating plug, b) frame of headphones with stimulating plugs, c) electrical stimulator, d) switching unit, e) common anode

into the EE such that each cathode was in contact with the predefined post at the EE. The reusable CE was crafted using a 2-mm-thick, 300-mm-long and 25-mm-wide ribbon made of highly water-absorptive sponge that was stitched below the stainless-steel mesh and Velcro tape. The geometric surface of the anode was approximately 7500 mm<sup>2</sup>. When wetted, the approximately 3-mm-thick anode contacted the skin as a homogeneous conductive solution. The components of the stimulating system are shown in **Figure 1**.

Despite the fact that the tANS was delivered via a battery-powered stimulator, tANS generated relatively large electric fields that propagated through the body towards the sensors of the measuring set-up. Fortunately, the sensors applied were out of the galvanic contact with the skin so the signals recorded could not be contaminated by electrical artefacts. To eliminate any potential interference, the neck was selected as the location to attach the CE and the subject grounded. Thus, the location was away from the sensors, and it separated galvanically the head from the body via thick bone and other tissues at a relatively small cross-section of the neck.

## 2.4 Measuring devices and procedures

To build the multi-channel measuring set-up, various custom-designed and commercially available devices were used. To capture heart sounds (PCG), two custom-developed transducers were used. Brachial arterial blood pressure (BABP) was measured using a pressure transducer and commercial blood-pressure appliance. To measure the forefinger pleths (FPPG), a pulse oximeter and an adult SpO<sub>2</sub> finger clip were used. To measure the toe pleths (TPPG), a pulse oximeter and customized photo-plethysmography foot clip were used. To record the blood flow in the brachial artery, the most advanced portable diagnostic ultrasound device was used. Signals were gathered using a high-performance I/O data-acquisition system and portable computer.

### 2.4.1 Auscultation of heart sounds

To capture the PCG that came from the heart valves, two custom-developed transducers shown in **Figure 2a** were used (frequency range 20–20,000 Hz, analogue voltage output 0.2–1 V). To distinguish types of sounds namely, S<sub>1</sub> and S<sub>2</sub>,<sup>18</sup> two transducers were placed at the standard heart auscultation positions shown in **Figure 3**. The first transducer was placed at the aortic heart auscultation position located at the 2<sup>nd</sup> right intercostal space of the ribs near the sternum. The second transducer was placed at the mitral or apex heart auscultation position located at the 5<sup>th</sup> left intercostal space of the ribs and in the middle of the clavicular line. To reduce the effect of high-frequency noises, the PCG signals were filtered using a low-pass filter (LPF) Butterworth, 10–300 Hz, 3<sup>rd</sup> with cut-off frequency of 300 Hz.<sup>19,20</sup> The transducers were used to potentially differentiate types of particular valve sounds that may be modified with the tANS. For

the calibration of both transducers, a portable sound-pressure calibrator (AWA6221A, Hangzhou Aihua Instruments Co., Ltd., Zhejiang, China) which provided a normal sound pressure level of 94 dB was used. The gain of each transducer was then trimmed until the same value as the normal sound-pressure level was obtained. The transducers were calibrated at room conditions of approximately 15 dB. For the frequency-response tests, however, a sine tone sweeping between 20 Hz and 1000 Hz was delivered to the transducers and the response was measured using the digital oscilloscope (InstruStar ISDS205A, Harbin ViMu Electronic Technology Co., Ltd., Harbin, China). To accomplish a FFT, the window-weighting function and range of waveform data that provided the best results in signal processing were selected. During the recording of heart sounds, the low-pass Butterworth filter at 1000 Hz was selected.

### 2.4.2 Measurement of brachial arterial blood pressure

The BABP was measured using a pressure transducer (Type 4-327-C, Range: 0–400 mmHg, Beckman Instruments Inc., Fullerton, CA, U.S.A.) shown in **Figure 2b**, that was situated serially between the proprietary cuff and commercial blood-pressure appliance (Oberarm-Blutdruckmessgerät MD 12450, salvatec, Essen, Germany). The appliance corresponds to standards for non-invasive blood-pressure measuring devices (EN 1060-1:1995+A1:2002 and EN 1060-3:1997+A1:2005). The pressure transducer and the appliance were calibrated occasionally using the reference values provided by a digital non-invasive sphygmomanometer calibrator (SLK-BXY-250, Shelok, Shaanxi, China). In an off-line analysis of the BABP trajectory, the value of the systolic blood pressure was taken from the trajectory at the point in which the first BABP oscillation was detected. The value of the diastolic pressure, however, was taken from the trajectory at the point at which the oscillation starts to disappear.

### 2.4.3 Measurement of forefinger photopleths

To measure the FPPG, a pulse oximeter (Nellcor N-595, Tyco Healthcare Group LP, Nellcor Puritan Bennett Division, Pleasanton, CA, U.S.A.) and an adult SpO<sub>2</sub> finger clip attached on the right forefinger (Nellcor DS-100A, Tyco Healthcare Group LP, Nellcor Puritan Bennett Division, Pleasanton, CA, U.S.A.) shown in **Figure 2c** were used.

### 2.4.4 Measurement of toe photopleths

To measure the TPPG, a pulse oximeter (Nellcor N-600, Tyco Healthcare Group LP, Nellcor Puritan Bennett Division, Pleasanton, CA, U.S.A.) instrumented with the customized photo-plethysmography foot clip shown in the **Figure 2d** was used. For this purpose, an IR/LED pair and photosensor were removed from the animal ear clip SpO<sub>2</sub> sensor (CSL032H, Oximax Animal Ear Clip SpO<sub>2</sub> Sensor for Nellcor N-595, Shenzhen YKD Technology Co., Ltd., Guangdong, China), was at-

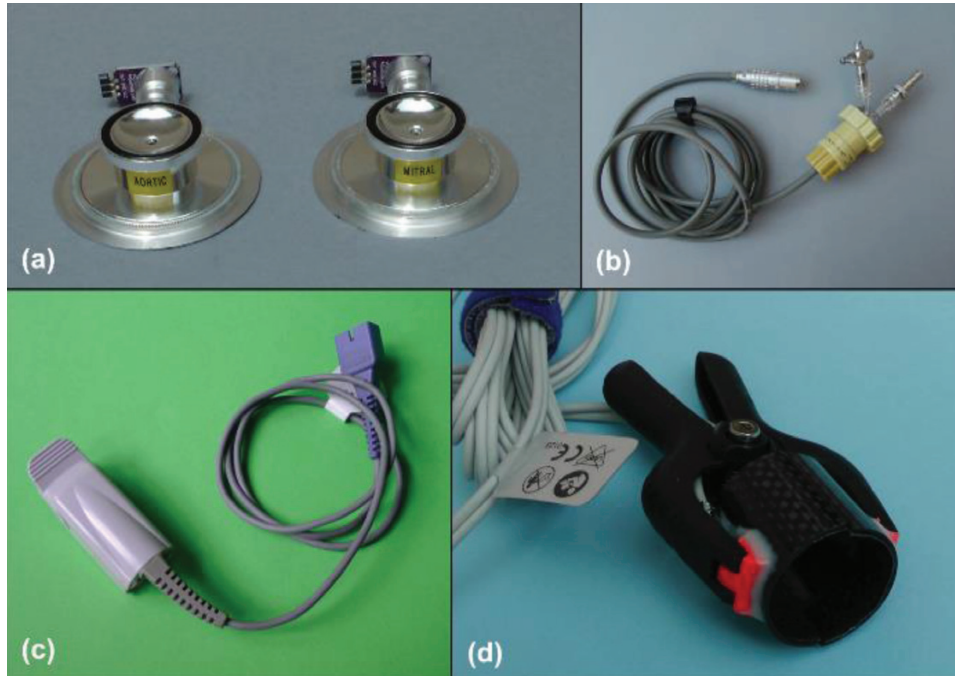


**Figure 2:** Measuring setup: a) Transducers for auscultation of phono-cardiographic signal, b) BABP pressure sensor, c) Forefinger clip SpO<sub>2</sub> sensor, d) Customized toe SpO<sub>2</sub> sensor

tached to the two halves of the tube made of carbon fibre so to face the lower and upper sides of the toe, respectively. By doing so, a photosensor of the toe clip was effectively shielded from direct light and the optical path from IR/LED pair to the photosensor was in an almost straight line. For the measurements, the foot clip was attached around the left toe.

#### 2.4.5 Measurement of pulsations in brachial artery

To record the blood flow in the brachial artery of the right arm in the first volunteer, two-dimensional (2-D) ultrasound mode (B), which uses the echo from solid structures to display 2-D images of the walls of blood vessels, was accomplished. For these purposes, the most advanced portable diagnostic ultrasound device (Venue Go™ Point of Care Ultrasound, ©GENERAL ELECTRIC COMPANY, U.S.A.), was used before and during the tANS. The transducer used was a linear array, which produced an array of parallel, high-frequency ultrasound while preserving detailed structural definition to a depth for the superficial brachial artery. The transducer was positioned along the brachial artery using water-soluble ultrasound transmission gel (UltrageL, AquaUltra Basic, UltrageL Hungary 2000 Ltd., Budapest, Hungary) and held in place. The position of the transducer was adjusted until the clearest picture was obtained. The instrument was then switched automatically to pulse wave Doppler mode and the mean velocity and cross-sectional luminal area were measured simultaneously. Accordingly, the diameter of arteries that varied with blood flow status and over the cardiac cycle, was displayed and recorded with motion. Records were then opened using the VLC media player free software and processed using

ImageJ-win64 software. Processing was performed within three steps: Extraction of frames at a specific interval opened with VLC software, Image analysis and Data processing. Results were used to construct diagrams showing a train of blood pulses expressed as vein cross-sectional area over time.

#### 2.4.6 Signal acquisition

All signals obtained from the conditioning circuits were gathered at 20 kHz with 24-bit resolution using a high-performance I/O data-acquisition system (DAC) (DEWE-43a, DEWESOFT d. o. o., Republic of Slovenia) as shown schematically in **Figure 3**. A DAC has eight differential analogue channel inputs and a USB 2.0 interface. The stimulating intensity  $i_c$  was assessed continuously by measurement of a voltage drop across the precision serial resistor of 10  $\Omega$  in the switching module connected to the stimulator output. During the acquisition, each signal was filtered using the low-pass filter that was selected based on the frequency band of the particular signal (see legend of **Figure 3**). Finally, data were stored on a portable computer (Lenovo W541, Lenovo, Beijing, China) to permit subsequent frequency analysis using software (DewesoftX). **Figure 3** shows a schematic diagram of the components comprising the system while the legend below **Figure 3** depicts the measured quantities and filtering applied.

#### 2.4.7 Experimental Procedures

A 45-minute trial was divided into four 5-minute sequences where  $i_c$  was delivered separately onto each of the four posts either at the left or the right EE, respec-

tively. The four sequences were separated with 5-minute shams where the tANS was not delivered onto any of positions. The 45-minute trial also started and ended with the 5-minute sham segment. Quantities  $i_c$ , APCG, MPCG, FPPG, and TPPG were acquired continuously throughout the entire trial. The BABP, however, was acquired approximately at the middle of each four 5-minute sequence.

The trials were carried out under the same (and as steady as possible) conditions with two healthy female volunteers, age 25 and 28. The subjects were instructed to avoid stress/tense and physical activity before the trial. Consumption of alcohol was prohibited before the trial. Consumption of a large meal later than an hour before the trial was prohibited. The subjects were asked to lay supine on the pedicure chair with arms at about heart level. The subjects were asked not to talk and to remain as still as possible. Stimulating and all testing positions

were degreased with 70 % isopropyl alcohol and allowed to dry. The subjects were instructed to relax and rest their elbows while the BABP cuff was wrapped around the left arm. Washers were adhered to the transducers. Transducers were placed at the two standard heart auscultation posts. A SpO2 clip sensor was attached to the right forefinger and placed on the left toe. Headphones with stimulating plugs were placed onto the head. The CA was placed on the neck. The intensity  $i_c$  of the stimuli delivered to the posts LW or RV was set at the level just below when discomfort was detected. Muscles in the vicinity of the brachial artery were relaxed so the mechanical limitation of instantaneous brachial arterial flow was avoided. The experiment was ended while minimizing  $i_c$  and turning the stimulator off. The subjects remained lying supine so stimulating and sensory components were removed. The skin at the EE posts and the skin at the cervical neck was degreased and dried.

#### 2.4.8 Offline Signal Analysis

Offline signal analysis was carried out using a portable computer (Lenovo W541, Lenovo, Beijing, China) and the aforementioned software DewesoftX. Any periods containing motion artefacts that could not be considered as captured signals were deleted. It was presumed that some potentially useful information about the state of the heart valves and arteries during and after tANS, would likely be obtained from the analysis. The BABP, FPPG, APCG, MPCG and TPPG, were analysed from traces during the BABP timeframe just before and just after the start of the tANS.

### 3 RESULTS

The results of the assessment are depicted in **Figure 4**, **Figure 5** and **Figure 6**. **Figure 4** depicts the relation-

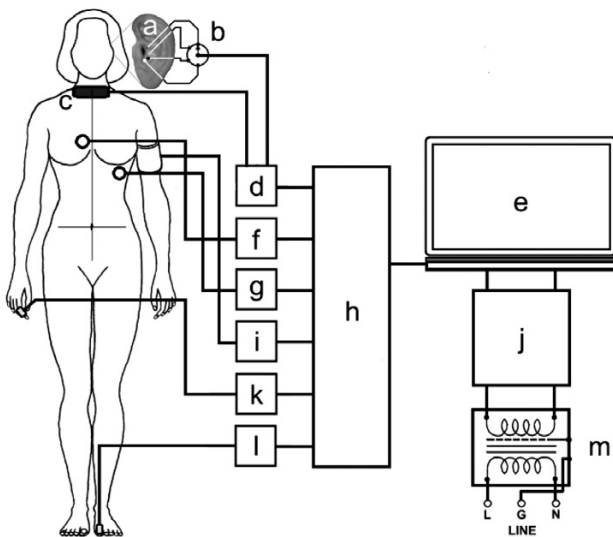


**Figure 3:** Schematic diagram of the experiment Legend

Mark	Devices and conditions	Input	Measured Signal	Symbol	Unit	Low Pass/Order
a	Stimulating posts R, Y, B, W	N/A	N/A	N/A	post	N/A
b	Stimulating post selector	N/A	N/A	N/A	selector	N/A
c	Common anode	N/A	N/A	N/A	anode	N/A
d	Electrical stimulator	0	tANS intensity	$i_c$	mA	Bessel, 1 kHz, 4th
e	Personal computer	N/A	N/A	PC	N/A	N/A
f	Auscultation transducer at aortic position	1	Aortic phono-cardiographic	APCG	dB	Butterworth, 10–300 Hz, 4th
g	Auscultation transducer at mitral position	4	Mitral phono-cardiographic	MPCG	dB	Butterworth, 10–300 Hz, 4th
h	Acquisition system	N/A	N/A	DAC	N/A	N/A
i	Pressure transducer at blood pressure appliance	7	Brachial artery blood pressure	BABP	mmHg	Bessel, 10 Hz, 4th
j	Power Supply Filter	N/A	N/A	N/A	N/A	N/A
k	Pulse oximeter I	9	Forefinger photo-plethysmographic	FPPG	mmHg	Bessel, 10Hz, 4th
l	Pulse oximeter II	14	Toe photo-plethysmographic	TPPG	mmHg	Bessel, 10Hz, 4th
m	Isolation transformer	N/A	N/A	N/A	N/A	N/A

ship between FPPG, TPPG, BABP, APCG and MPCG, before and during the tANS.<sup>9,21</sup> Precisely, the results are represented through waveforms of the quantities APCG, MPCG, BABP, FPPG and TPPG that were recorded in the second volunteer before and during the tANS of the post LW located at the bottom of the left EE. **Table 1** shows vascular time interval VTT1 elapsed between the first heart sound S1 and vascular time interval VTT2 elapsed between the second heart sound S2 and systolic peak in the FPPG signal before the tANS, vascular time interval VTT3 elapsed between the first heart sound S1 and vascular time interval VTT4 elapsed between the second heart sound S2 and systolic peak in the FPPG signal during the tANS. **Table I** also shows a vascular time interval VTT1 elapsed between the first heart sound S1 and vascular time interval VTT2 elapsed between the second heart sound S2 and systolic peak in the TPPG signal before the tANS, vascular time interval VTT3 elapsed between the first heart sound S1 and vascular time interval VTT4 elapsed between the second heart sound S2 and systolic peak in the TPPG signal during the tANS.

Similarly, **Figure 5** depicts the relationship between FPPG, TPPG, BABP, APCG and MPCG, before and during the tANS.<sup>9</sup> The results are represented through wave-

forms of the quantities APCG, MPCG, BABP, FPPG, and TPPG that were recorded in the second volunteer before and during the tANS of the post RW located at the bottom of the right EE. **Table 1** shows vascular time interval VTT1 elapsed between the first heart sound S1 and vascular time interval VTT2 elapsed between the second heart sound S2 and systolic peak in the FPPG signal before the tANS, vascular time interval VTT3 elapsed between the first heart sound S1 and vascular time interval VTT4 elapsed between the second heart sound S2 and systolic peak in the FPPG signal during the tANS. **Table I** also shows a vascular time interval VTT1 elapsed between the first heart sound S1 and vascular time interval VTT2 elapsed between the second heart sound S2 and systolic peak in the TPPG signal before the tANS, vascular time interval VTT3 elapsed between the first heart sound S1 and vascular time interval VTT4 elapsed between the second heart sound S2 and systolic peak in the TPPG signal during the tANS.

**Figure 6** shows an ultrasound image of pulsing the right brachial artery indicated with arrows, and a train of pulsing vein cross-sectional area over time in the first volunteer. **Figure 6a** shows the brachial artery pulsing without tANS, while **Figure 6b** shows brachial artery pulsing with tANS of the W post at the left EE. Finally,

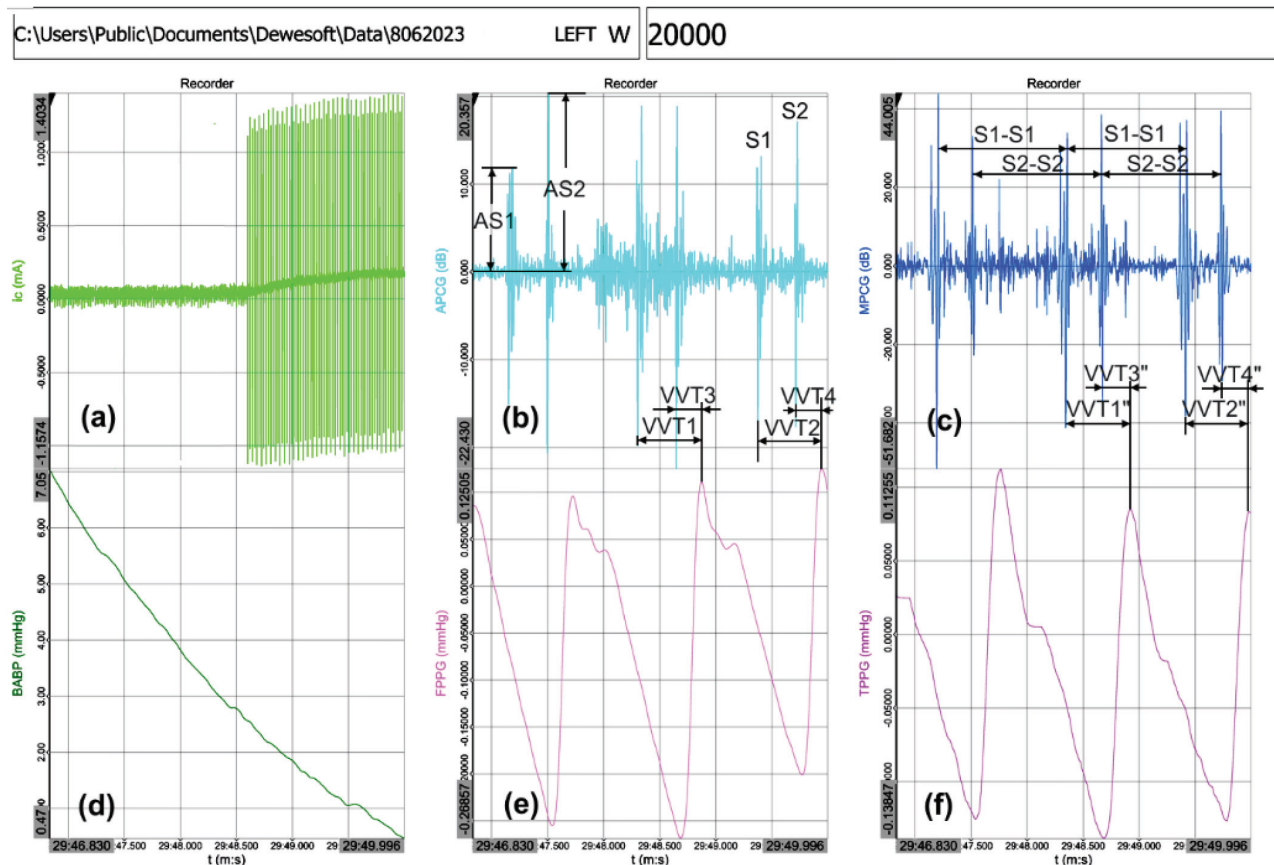


**Figure 4:** Relationship between APCG and MPCG, FPPG and TPPG, vascular time interval VTT1 between the first heart sound S1, vascular time interval VTT2 between the second heart sound S2, and the corresponding systolic peak in the FPPG and TPPG signals before and during multipost tANS of the LW in the second volunteer. Recorded quantities: a)  $i_c$ , b) APCG, c) MPCG, d) BABP, e) FPPG, and f) TPPG.

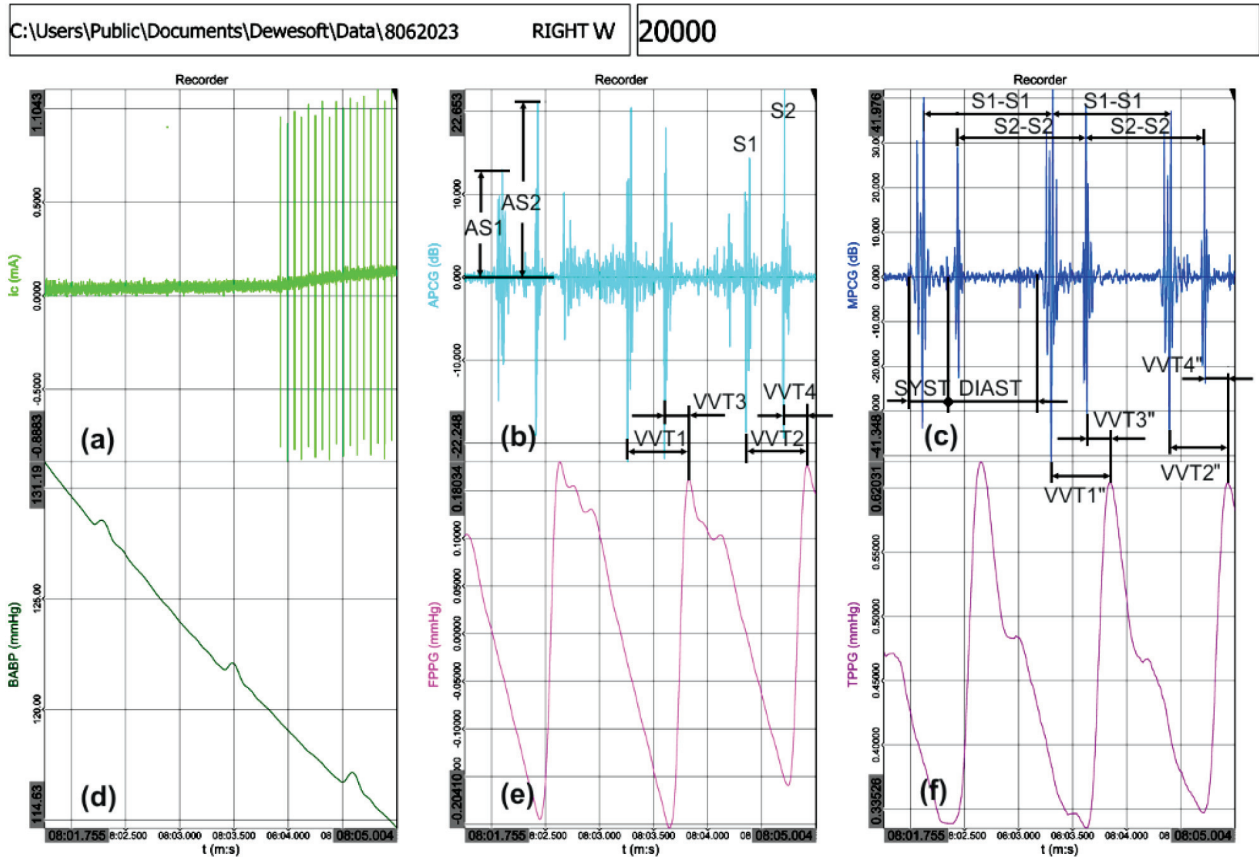


**Figure 5:** Relationship between APCG and MPCG, FPPG and TPPG, vascular time interval (VVT1) between the first heart sound S1, vascular time interval (VVT2) between the second heart sound S2, and the corresponding systolic peak in the FPPG and TPPG signals before and during multipost tANS of the RW in the second volunteer. Recorded quantities: a)  $i_c$ , b) APCG, c) MPCG, d) BABP, e) FPPG, and f) TPPG.

**Table 1:** Vascular time intervals between heart sounds and systolic peaks, heart-sound amplitudes and heart-cycle durations in the second volunteer before and during the tANS, respectively.

HEART SOUND	PHOTOPLETHISMOGRAM	MARK	LEFT EE POST W		EFFECT	RIGHT EE POST W		EFFECT
			WITHOUT tANS	WITH tANS		WITHOUT tANS	WITH tANS	
APCG	FPPG	VVT1	568,67 [ms]	-	↑	567,93 [ms]	-	↑
		VVT2	-	577,96 [ms]		-	568,25 [ms]	
		VVT3	225,71 [ms]	-		227,11 [ms]	-	
		VVT4	-	234,75 [ms]		-	227,43 [ms]	
		AS1	10,843 [dB]	21,849 [dB]	↑	20,432 [dB]	14,307 [dB]	↓
		AS2	20,177 [dB]	20,989 [dB]	↑	17,915 [dB]	22,43 [dB]	↑
		S1-S1	679,91	727,22	↑	1193 [ms]	1102 [ms]	↓
		S2-S2	687,89	695,59	↑	1182 [ms]	1102 [ms]	↓
MPCG	TPPG	VVT1''	587 [ms]	-	↓	545,38 [ms]	-	↓
		VVT2''	-	568,92 [ms]		-	545,31 [ms]	
		VVT3''	252,83 [ms]	-		215,73 [ms]	-	
		VVT4''	-	243,79 [ms]		-	204,69 [ms]	
		AS1	39,269 [dB]	44,564 [dB]	↑	41,496 [dB]	37,148 [dB]	↓
		AS2	32,154 [dB]	43,864 [dB]	↑	38,502 [dB]	30,152 [dB]	↓
		S1-S1	684,76	708,41	↑	1193 [ms]	1090 [ms]	↓
		S2-S2	684,76	700,72	↑	1182 [ms]	1102 [ms]	↓

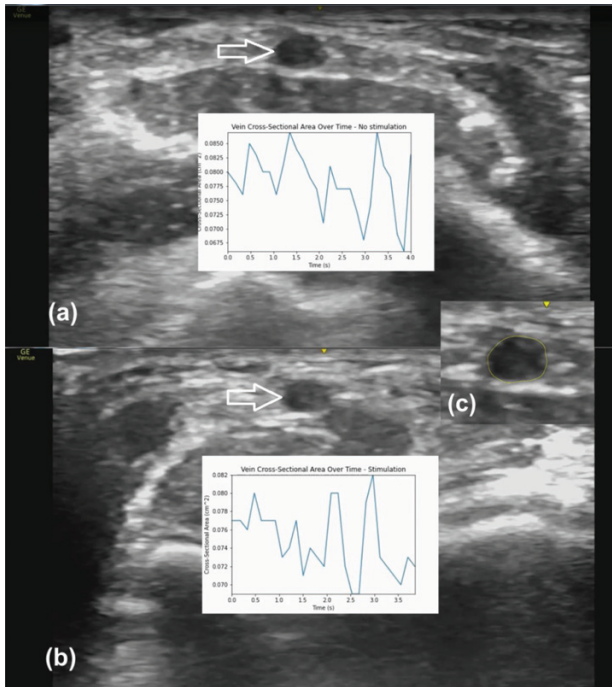


**Figure 6:** Ultrasound image of the right Brachial artery pulsing and vein cross-sectional area over time in the first volunteer: a) without tANS, b) with tANS of the RW post, c) Phase of processing

**Figure 6c** shows the encircled vein as an important processing step of both video recordings.

#### 4 DISCUSSION

In this study we evaluated the effects of multipost tANS on the dynamics in heart activity and blood flow in two volunteers during tANS at predefined posts of the EE and listed potential effects on related hemodynamic functions. The overall hypothesis of the study was that the tANS of predefined posts on the left and right EE can have a measurable effect on heart sounds and some hemodynamic functions in healthy female volunteers.

The main difference between our study and the studies of others is that in our study the tANS can be delivered to posts on the EE via multiple combinations of four electrodes mounted at predefined positions on a silicone plug.<sup>22</sup> In addition, optimum working electrochemical conditions of platinum cathodes used for the tANS were well defined considering Faradaic reactions as shown in Section 2.3 tANS set-up. As a result, skin irritation at the tANS posts was never observed. Furthermore, the charge density injected by the CE was lower than that injected by the cathode, so skin irritation stimulating effects were never observed.

The greatest weakness of the paradigm, however, was that  $i_c$  density and tANS efficiency were both dependent predominantly on the pressure produced by the silicone plug and less on small changes in the position of the plug within the EE.<sup>23</sup> Furthermore, trials were carried out and analysed by the same investigator, which might have re-

sulted in some biases. However, the numerical data of the captured signals based on offline signal analysis shown in **Table 1**, minimized subjective interpretation. The study was intended mainly to obtain initial information on the efficiency of the multipost tANS so the number of subjects tested and measurements performed were low. Accordingly, the results obtained should be considered as a basis to gain further research activities that may result in clinically valuable conclusions. A discussion on the particular entity measured is presented below.

Body sounds contain important information about human physiological and psychological conditions.<sup>24</sup> A non-invasive capture of biomedical signals is relatively simple and inexpensive; however, body sounds are usually barely audible. Most contact transducers available are capable of capturing body sounds that are mainly located within the frequency spectrum, ranging from 20 Hz to 1.3 kHz.<sup>25</sup> Besides, the loudness of captured heart sounds varies with the auscultation positions.<sup>26</sup> However, modern biomedical signal-processing techniques are able to accurately characterize significant features of the heart sounds contained within the PCGs.<sup>27</sup> With this relation, the captured S1 and S2 sound can be used to determine the heart sound type and to detect potentially modified heart sounds. The amplitude of S1 may provide some valuable information about myocardial contractility ability.<sup>28</sup> It was shown that transducers developed enabled a high-quality auscultation of S1 and S2. The hypothesis that the tANS has a measurable effect on heart sounds was confirmed.

An artery of interest for the work was the brachial artery as the major blood vessel of the upper arm. It was presumed that tANS can elicit a measurable difference in the BABP pressure. This hypothesis was not confirmed.

Results showed that vascular time intervals VVT1, VVT2, VVT3 and VVT4 between heart sounds S1 and S2, captured as APCG and systolic peaks measured as FPPG in the second volunteer, were slightly larger during the separate tANS of both posts, once for the LW and once for the RW than before the tANS. It was also shown that during the tANS of the LW post, heart cycles S1-S1 and S2-S2 contained within the APCG, became slightly larger and, thus, the heart rhythm became slightly lower. Besides, they both became slightly louder. During the tANS of the RW post, however, heart cycles S1-S1 and S2-S2 contained within the APCG, became slightly smaller and, thus, the heart rhythm became slightly higher. Furthermore, S1 became slightly quieter while S2 became slightly louder. The hypothesis that tANS of the LW and RW has a measurable effect on the forefinger photoplethysmography was confirmed.

Results showed that vascular time intervals VVT1", VVT2", VVT3" and VVT4" between heart sounds S1 and S2, captured as MPCG and systolic peaks measured as TPPG in the second volunteer, were slightly smaller during the separate tANS of both posts, once for the LW and once for the RW than before the tANS.

It was also shown that during the tANS of the LW post, heart cycles S1-S1 and S2-S2 contained within the MPCG became slightly larger and, thus, the heart rhythm slightly lower. Besides, both heart sounds S1 and S2 became louder. During the tANS of the RW post, however, heart cycles S1-S1 and S2-S2 contained within the MPCG, became slightly smaller and, thus, the heart rhythm became slightly higher. Furthermore, both, S1 and S2 became slightly quieter. The hypothesis that tANS of the LW and RW has a measurable effect on the toe photoplethys was confirmed.

The paper details how changes in pulsations of the brachial artery potentially elicited with the tANS were obtained using an ultrasound transducer. The exact dynamics between the brachial artery pulsations and blood pressure are actually complex. Namely, blood vessels have viscoelastic properties that allow the diameter to vary with a pulsating pressure generated by the left ventricle contractions. It was shown in **Figure 6a** that the pattern of the right brachial artery pulsing expressed with a train of pulsing vein cross-sectional area over time without tANS, was different to the brachial artery pulsing with tANS of the W post at the left EE. It was also shown that the pattern of the proprietary vein cross-sectional area over time with tANS was different compared to both the FPPG and TPPG. Accordingly, the hypothesis that tANS has a measurable effect on pulsations in the brachial artery was confirmed.

Previous studies have indicated that the performance and autonomic function could be enhanced with the tANS and that tANS may be a promising treatment for some neuropsychiatric disorders.<sup>29,30</sup> With this relation the directions of our future work can include tANS using a matrix of electrodes and multiple combinations of electrodes to stimulate multiple posts on the EE and fine-tuning of the tANS parameters.<sup>22</sup>

## 5 CONCLUSIONS

It was shown that differences in all vascular time intervals and heart-cycle durations, obtained without tANS and with tANS of both posts, the LW and RW, were actually small but were consistent.

It can be concluded that tANS of the LW post elicited slightly lower heart rate than the one measured when LW was not stimulated. In contrast, it can be concluded that the tANS of the RW post elicited a slightly higher heart rate than the one measured when RW was not stimulated.

Accordingly, the research involving tANS can promote the method potentially useful to re-establish imbalance or lack of autonomic nervous modulation of heart valve function. One particular challenge arose from the study was to determine if valvar motion during diastole and/or systole is influenced by the innervation that was modulated by the multipost tANS.

However, to place a methodology into service in a clinical environment, it should be tested in a larger group of subjects and trials.

## Acknowledgement

The authors wish to acknowledge the Program team (Research core funding No. P3-0171 by the Slovenian Research and Innovation agency, Ministry of Higher Education, Science and Innovation, Republic of Slovenia) at the Institute of Pathophysiology, Faculty of Medicine, University of Ljubljana, Republic of Slovenia for providing language help, writing assistance, proof reading the article and editing the manuscript.

## 6 REFERENCES

- J. T. Mortimer, N. Bhadra, *Fundamentals of Electrical Stimulation*, In: Krames ES, Peckham PH, Rezai Ali R, editors, *Neuromodulation*, Academic Press; 2009, 109–121. doi:10.1016/B978-0-12-374248-3.00012-4
- J. Ellrich, *Transcutaneous vagus nerve stimulation*, *Eur. Neurol. Rev.*, 6 (2011) 4, 254–6, doi:10.17925/ENR.2011.06.04.254
- W-P. Teo, M. Muthalib, S. Yamin, A. M. Hendy, K. Bramstedt, E. Kotsopoulos, S. Perrey, H. Ayaz, *Does a combination of virtual reality, neuromodulation and neuroimaging provide a comprehensive platform for neurorehabilitation? A narrative review of the literature*, *Frontiers in Human Neuroscience*, 10 (2016) 284, doi:10.3389/fnhum.2016.00284
- B. W. Badran, L. T. Dowdle, O. J. Mithoefer, N. T. LaBate, J. Coatsworth, J. C. Brown, W. H. DeVries, C. W. Austelle, L. M. McTeague, M. S. George, *Neurophysiologic effects of transcutaneous auricular vagus nerve stimulation (taVNS) via electrical stimulation of the tragus: A concurrent taVNS/fMRI study and review*, *Brain Stimul.*, 11 (2018) 3, 492–500, doi:10.1016/j.brs.2017.12.009
- B. W. Badran, O. J. Mithoefer, C. E. Summer, N. T. LaBate, C. E. Glusman, A. W. Badran, W. H. DeVries, P. M. Summers, C. W. Austelle, L. M. McTeague, J. J. Borckardt, M. S. George, *Short trains of transcutaneous auricular vagus nerve stimulation (taVNS) have parameter-specific effects on heart rate*, *Brain Stimul.*, 11 (2018) 4, 699–708, doi:10.1016/j.brs.2018.04.004
- M. A. A. Hamid, M. Abdullah, N. A. Khan, Y. M. A. AL-Zoom, *Biotechnical System for Recording Phonocardiography*, *International Journal of Advanced Computer Science and Applications (IJACSA)*, 10 (2019) 8, doi:10.14569/IJACSA.2019.0100864
- A. Ramović, L. Bandić, J. Kevrić, E. Germović, A. Subasi, *Wavelet and Teager energy operator (TEO) for heart sound processing and identification*, In: *CMBEBIH 2017*, Springer; 2017, 495–502. <https://www.healio.com/cardiology/learn-the-heart/cardiology-review/topic-reviews/heart-sounds>
- Learn The Heart. Cardiology Review, Topic Reviews A-Z, Heart Sounds Topic Review*, <https://www.healio.com/cardiology/learn-the-heart/cardiology-review/topic-reviews/heart-sounds>, 20.06.2023
- V. N. Varghees, K. I. Ramachandran, *A novel heart sound activity detection framework for automated heart sound analysis*, *Biomedical Signal Processing and Control*, 13 (2014), 174–188, doi:10.1016/j.bspc.2014.05.002
- T. H. Chowdhury, K. N. Poudel, Y. Hu, *Time-Frequency Analysis, Denoising, Compression, Segmentation, and Classification of PCG Signals*, *IEEE Access*, 8 (2020) 160882–160890, doi:10.1109/ACCESS.2020.3020806
- Y. Henderson, F. E. Johnson, *Two modes of closure of the heart valves*, *Heart*, 4 (1912), 69–82

- <sup>12</sup>X. Hu, Q. Zhao, X. Ye, Autonomic regulation of mechanical properties in porcine mitral valve cusps, *Arq. Bras. Cardiol.*, 98 (2012) 4, 321–8, doi:10.1590/s0066-782x2012000400006. PMID: 22735910
- <sup>13</sup>A. Jubran, Pulse oximetry, *Crit Care*, 19 (2015) 1, 272, doi:10.1186/s13054-015-0984-8
- <sup>14</sup>M. Elgendi, R. Fletcher, Y. Liang, N. Howard, N. H. Lovell, D. Abbott, K. Lim, R. Ward, The use of photoplethysmography for assessing hypertension, *npj Digit. Med.* 2 (2019) 60, doi:10.1038/s41746-019-0136-7
- <sup>15</sup>P. Bonham, Measuring toe pressures using a portable photoplethysmograph to detect arterial disease in high-risk patients: an overview of the literature, *Ostomy Wound Manage.* 57 (2011) 11, 36–44
- <sup>16</sup>Cleveland Clinic. Hemodynamic Test, <https://my.clevelandclinic.org/health/diagnostics/17094-hemodynamic-test>, 20.06.2023
- <sup>17</sup>J. P. Jamison, A. Campbell, C. Devlin, C. D. Johnson, Brachial artery blood flow by vascular ultrasound in education, *Adv. Physiol. Educ.*, 46 (2022), 498–506, doi:10.1152/advan.00157.2021
- <sup>18</sup>A. Bhaskar, A simple electronic stethoscope for recording and playback of heart sounds, *Adv. Physiol. Educ.*, 36 (2012), 360–362, doi:10.1152/advan.00073.2012
- <sup>19</sup>A. M. Noor, M. F. Shadi, The heart auscultation. From sound to graphical, *Journal of Engineering and Technology (JET)*, 4 (2013) 2, 73–84
- <sup>20</sup>C. N. Gupta, R. Palaniappan, S. Rajan, S. Swaminathan, S. M. Krishnan, Segmentation and classification of heart sounds, *Proc. of the Can. Conf. Electrical Comput. Eng.*, Saskatoon 2005, 1674–1677, doi:10.1109/CCECE.2005.1557305
- <sup>21</sup>M. Nitzan, B. Khanokh, Y. Slovik, The difference in pulse transit time to the toe and finger measured by photoplethysmography, *Physiol. Meas.*, 23 (2002) 1, 85–93. doi:10.1088/0967-3334/23/1/308
- <sup>22</sup>B. W. Badran, J. C. Brown, L. T. Dowdle, O. J. Mithoefer, N. T. LaBate, J. Coatsworth, W. H. DeVries, C. W. Austelle, L. M. McTeague, A. Yu, M. Bikson, D. D. Jenkins, M. S. George, Tragus or cyma conchae? Investigating the anatomical foundation of transcutaneous auricular vagus nerve stimulation (taVNS), *Brain Stimul.*, 11 (2018) 4, 947–948, doi:10.1016/j.brs.2018.06.003
- <sup>23</sup>B. W. Badran, A. B. Yu, D. Adair, G. Mappin, W. H. DeVries, D. D. Jenkins, M. S. George, M. Bikson, Laboratory Administration of Transcutaneous Auricular Vagus Nerve Stimulation (taVNS): Technique, Targeting, and Considerations, *J. Vis. Exp.*, 143 (2019), e58984, doi:10.3791/58984
- <sup>24</sup>M. Elgendi, TERMA Framework for Biomedical Signal Analysis: An Economic-Inspired Approach, *Biosensors*, 55 (2016) 6(4), doi:10.3390/bios6040055
- <sup>25</sup>T. Rahman, A. T. Adams, M. Zhang, E. Cherry, B. Zhou, H. Peng, T. Choudhury, BodyBeat: a mobile system for sensing nonspeech body sounds, *Proc. of the 12th annual international conference on Mobile systems, applications, and services*, Bretton Woods 2014, 2–13, doi:10.1145/2594368.2594386
- <sup>26</sup>M. McGregor, M. B. Rappaport, H. B. Sprague, A. L. Friedlich, The calibration of heart sound intensity, *Circulation*, 13 (1956) 2, 252–256., doi:10.1161/01.cir.13.2.252
- <sup>27</sup>W. C. Kao, C. C. Wei, Automatic phonocardiograph signal analysis for detecting heart valve disorders, *Expert Systems with Applications*, 38 (2011) 6, 6458–6468, doi:10.1016/j.eswa.2010.11.100
- <sup>28</sup>A. Subasi, Chapter 2-Biomedical Signals, Editor(s): Abdulhamit Subasi, *Practical Guide for Biomedical Signals Analysis Using Machine Learning Techniques*, Academic Press, 2019, 27–87, doi:10.1016/B978-0-12-817444-9.00002-7
- <sup>29</sup>J. A. Clancy, D. A. Mary, K. K. Witte, J. P. Greenwood, S. A. Deuchars, J. Deuchars, Non-invasive vagus nerve stimulation in healthy humans reduces sympathetic nerve activity, *Brain Stimul.*, 7 (2014) 6, 871–7, doi:10.1016/j.brs.2014.07.031
- <sup>30</sup>L. V. Borovikova, S. Ivanova, M. Zhang, H. Yang, G. I. Botchkina, L. R. Watkins, H. Wang, N. Abumrad, J. W. Eaton, K. J. Tracey, Vagus nerve stimulation attenuates the systemic inflammatory response to endotoxin, *Nature*, 405 (2000) 6785, 458–62, doi:10.1038/35013070